Condition monitoring of press-pack IGBT devices using Deformation Detection Approach

Bowen Gu[1*], Haimeng Wu[1,2], Volker Pickert[1], Siyang Dai[3], Zhiqiang Wang[3], Guofeng Li[3], Shuai Ding[4], Bing Ji[4]

[1] *School of Engineering Newcastle University Newcastle upon tyne UK*
[2] *Department of Mathematics, Physics and Electrical Engineering, Northumbria University, Newcastle, UK*
[3] *Faculty of Electronic Information and Electrical Engineering Dalian University of Technology CHINA*
[4] *School of Engineering University of Leicester UK*
Email: b.gu2@newcastle.ac.uk

Keywords: PRESS-PACK IGBT, THERMAL-MECHANICAL, RELIABILITY, DEFORMATION, FIBER BRAGG GRATING (FBG)

Abstract

Press pack Insulated Gate Bipolar Transistors (PP IGBT) are gaining more attention in HVDC power transmission systems due to their high-power density and high reliability compared with conventional power modules. Condition monitoring of PP IGBTs is normally conducted by estimating the chip temperature which is challenging to implement in practice. This paper presents a new parameter, deformation of the upper lid groove, to indicate the health condition of the PP IGBT based on its unique packaging technique. The thermal-mechanical coupled model is built by FE software in order to investigate the relationship between the deformation and junction temperature of the chips. In addition, the several feasible detection methods of deformation have been discussed and utilization of the fiber Bragg grating (FBG) sensor shows the advantages as the most appropriate approach, which can be further developed for condition monitoring using deformation measurements.

1 Introduction

With the development of clean and renewable energy, High-Voltage Direct Current (HVDC) power transmission technology plays a significant role in the energy transmission process between the power source and power grid. Over one hundred HVDC systems have been installed globally with more than 20 new designed projects built in the last decade [1-2]. Thus, an increasing demand for high reliable power semiconductors for these applications are required. However, conventional Insulated Gate Bipolar Transistor (IGBT) power modules using bond wire and soldering technique are seen as unreliable for HVDC because of solder crack and bond wire lift off failures. In contrast, PP-IGBTs have a unique structure without utilizing bond wire connection and soldering, thereby, such kind of device has many merits in terms of reliability, power density and heat dissipation ability and it is therefore widely used in HVDC transmission system [3-4].

In the past, research on PP-IGBT devices focused on the analysis of physical changes in the press-pack properties caused by mechanical and thermal stress. To establish these changes, a physical model in finite element are simulated. S. Dai conducted a 3D FEM approach to numerically simulate the mechanical clamping conditions of the static thermal distribution of IGBT chips. C. Huifeng et al. carried out a CFD simulation that focuses on the coolant channels design for the heatsink of PP IGBT to minimize the temperature propagation [6]. T. Poller et al. [7] investigated the influence of clamping force on the electrical contact resistance and thermal contact resistance. To validate simulation results, various tests have been conducted. Power cycling tests reveal two possible failure modes: the damage of the gate-oxide and the micro eroding between the die and molybdenum plate [8]. Another research reports the influence of the pressure between the chip layer and molybdenum plate, where a very high mechanical pressure can result in the mechanical damage of the chip, but if the mechanical pressure is too low it can cause sudden rise of the chip junction temperature [9]. Overall, the clamping force is one of the most important parameters which affects the reliability of PP-IGBTs and this has been studied widely [10]. Condition monitoring on PP-IGBTs is less researched compared to its counterpart, the conventional power module. A list of different condition monitoring techniques including its sensor requirements for conventional power modules is shown in [11]. In [13], condition monitoring on PP-IGBTs is conducted by applying the plasma-extraction transit-time (PETT) method to detect the temperature, and a controllable and flexible PETT oscillation characteristics was carried out. In [13], the overall fatigue of PP-IGBT device was analyzed but no detailed condition monitoring circuit was suggested.

In this paper, a coupled physical model under thermal-mechanical field is established and the static FE simulation under different power dissipation conditions are studied. The results show that the uneven pressure distribution affects the thermal distribution of the chips and the difference of temperature affects the tight fit between the different layers of PP-IGBTs. Subsequently this causes an uneven pressure distribution in the lid of the press-pack which in turn leads to the occurrence of deformation of the lid. The paper identifies the area that shows the largest deformation in the lid which is the groove. Simulation results show the contribution of deformation caused by the pressure from the power dissipation of the chips and caused by the clamping pressure. Knowledge gained from this work lead to a new condition monitoring parameter: the deformation of the groove in the lid of the press-pack. The paper proposes and compares several detection methods and analyze them against selected parameters such as accuracy, sensitivity and practicality.

2 Principle and modelling

At present, two bond wire-less structures of press pack technology are commercially available on the market. The most commonly used structure is using rigid pillars with the

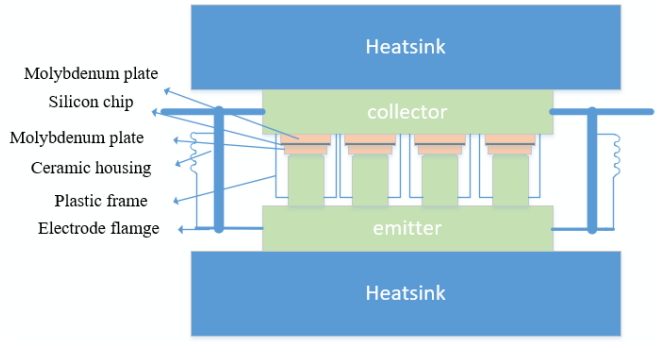

(a)

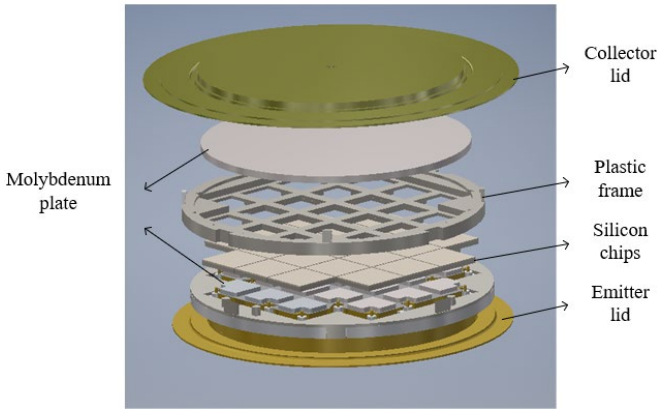

(b)

Fig. 1 (a) Schematic structure of PP-IGBT device with the hard crimping and (b) the developed physical model in FE software

hard-crimping technology [14]. The other type of structure is applying the spring-type crimping technology IGBT which

can balance the pressure unevenness to a certain extent [15]. In this paper, the simulation of the thermal-mechanical model and the deformation analysis have been carried out based on rigid pillars PP-IGBTs. The schematic structure and the developed physical model in FE are shown in Fig.1.

As illustrated in Fig.1, the structure can be defined as five layers which consists of two molybdenum plates, two copper lids and a die in the middle. The collector side of the die connects to the cooper lid via a molybdenum plate, and the emitter side of the chip connects to the copper lid via the molybdenum plate and the copper pillar in order to form thermal and electrical contact. The gate distribution board is connected to the die through a spring-loaded pin and the entire construction is placed in a hermetical capsule. Clamping force is utilized in order to achieve the thermal and electrical contact in PP-IGBTs which is different with the conventional IGBT modules using the soldered wire bond.

In order to monitor the condition of the rigid pillars PP-IGBTs, the link between the temperature of the chips and the deformation needs to be established since the thermal stress failure of the chip is the most common factor for the destruction of a semiconductor device. In this work, the temperature distribution is generated under power loss and

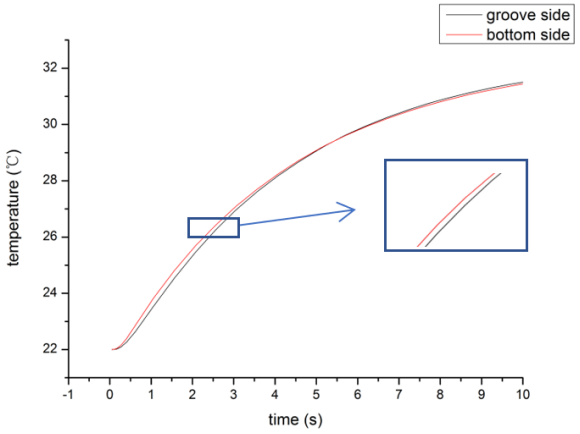

Fig. 2 Time cost of heat transfer cross the lid

affected by the mechanical stress constraint. The deformation and mechanical strain are produced by clamping force and changed with thermal fluctuation. Equation (1) demonstrates the temperature calculation transferred from the

initial power loss, where ρ is the density, C_p is the specific heat capacity, k is the thermal conductivity, and Q is the heat flux. T is temperature function with position x and time t. The value of the parameters is shown in Table 2. Temperature is the crucial parameter in the physical model since it affects the mechanical and electrical performance.

$$C_p\rho\frac{\partial}{\partial t}T(x,t) - k\Delta T(x,t) = Q \quad (1)$$

To analysis the deformation in the mechanical field, two kinds of strain are included. The elastic strain and plastic strain based on the material properties and the thermal strain that changed with temperature fluctuation. Equations (2) and (3) explain the basic principle of strain generation, where E is Young's Modulus, $\sigma$is stress, $\varepsilon$is strain, which is the function with temperature T.

$$\sigma = E\varepsilon \quad (2)$$

$$\varepsilon = \alpha\Delta T \quad (3)$$

Fig. 2 shows the amount of time of heat transfer from the top side in the device to the bottom side of the upper lid. As heat accumulation is a slow process, according to the figure above, the time consumption of reaching the same temperature for both sides is in seconds level and the deformation can characterize the changes of the average temperature. Therefore, judging the temperature through deformation is acceptable.

3 Simulation verification

In order to improve the computational efficiency, the plastic frame and the gate signal distribution board are not considered in this developed model. The FE simulation is carried out in ANSYS by using the static thermal and structure tools. Meshing size is chosen as 1mm to get better results and high computational speed at the same time. The room temperature is set to 22℃. The dimensions and the material of each

Table 1 Material and dimensions of the components inside the device

Component	Thickness (mm)	Surface area (mm^2)
Si chip	0.58	64
Collector Mo plate	1.3	64
Emitter Mo plate	1.1	64
Pillar	8.5	64
Collector pole	11	1735
Emitter pole	7.2	1735

Table 2 Material properties in the simulation model

Material	Silicon	Molybdenum	Copper
k [W/(m*K)]	148	130	385
α (1/°C)	4.8E-06	4.9E-06	1.71E-05
E (GPa)	162	320	129
σ	0.23	0.28	0.34
ρ (kg/m^3)	2330	10220	8933

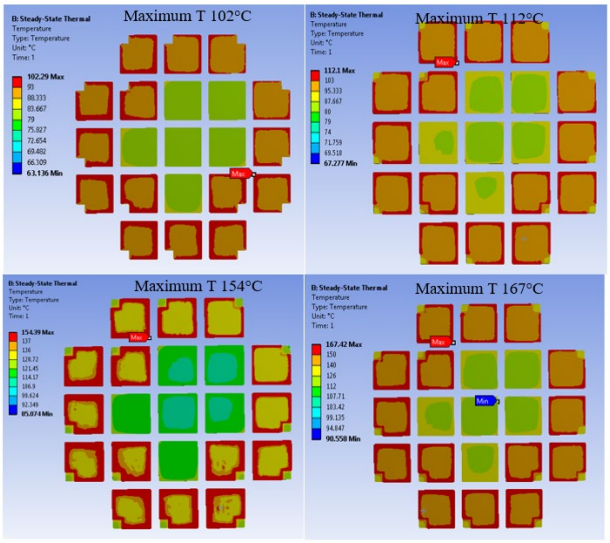

(a)

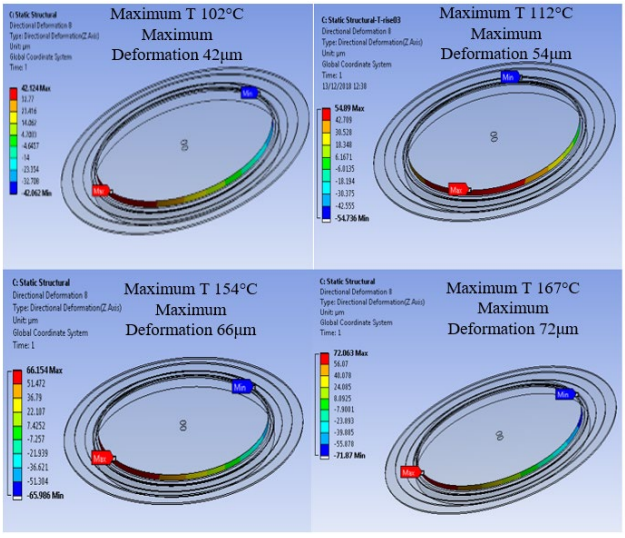

(b)

component used for the device are essential information to establish the model and Table 1 shows these parameters applied in the model.

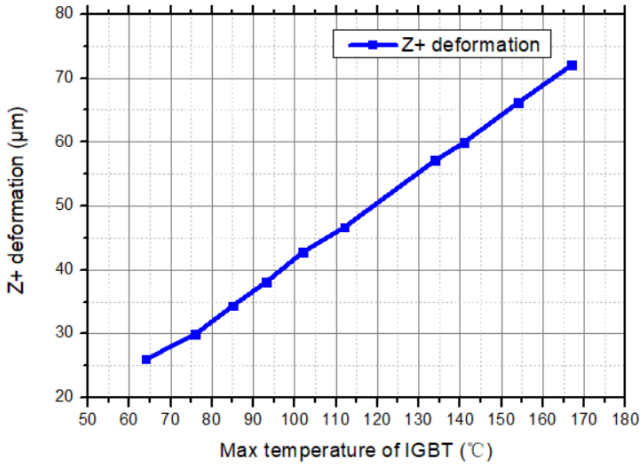

(c)

Fig. 3 simulation results (a) temperature distribution across the chip surface (b) deformation against temperature of the upper lid groove (c) relationship between the temperature and deformation

Table 2 presents the required material properties in the simulation model, where k is the coefficient of thermal conductivity, ρ is the material density, α is the coefficient of thermal expansion, E is the Young's module and σ is the Poisson ratio.

To analyze the deformation, the static FE simulation based on thermal-mechanical model is carried out and the average temperature is applied as one factor to generate the deformation. In this study, the PP IGBT operates under steady current energized with no other loss and the constraints are described as follows. The impact of electrical field for deformation is considered as the power dissipation from each chip which generates the heat. The convection heat transfer coefficient between different layers are all set based on practical situation. Two heat sinks are included in the simulation, the even clamping force is set on the surface of collector side heat sink and the other side is fixed support. All the contact surfaces among different layers within PP-IGBT are assumed to be friction contact except the contact between the heat sink and the device since these two surfaces are relatively smooth. The selected model using in this work has 21 chips in total, 15 IGBT chips in the outer ring, 6 diodes in the middle part. Different power dissipation is set to the IGBT chips and diodes based on the datasheet.

Considering the practical condition, the analysis of the deformation is mostly focused on the groove of the upper copper lid. Fig. 3 (a) shows the temperature distribution of chips on the collector side when the power dissipation of the IGBT die is set from 2500 to 3600 pw/μm^3. The maximum temperature increases from 102°C to 167°C. It can be seen that the IGBT chips on the outer ring have higher temperature compared with diode chips owing to the different power loss. In addition, higher temperature trends at the edge of each chip. Fig.3 (b) presents the Z axis deformation of the lid groove according to Fig. 3 (a), the amount of the deformation ranges from 42 μm to 72 μm at the maximum point. Fig.3 (c) shows the relationship between the temperature and deformation.

Table 3 Deformation Sensors

No.	Sensor	Sensitivity	Immunity	Complexity
1	Strain gauge sensor [16]	GF=2	poor	Wheastone bridge
2	Long-gauge-length fibre-optical sensor [21]	2μm	high	Need reading unit
3	ESPI (Electronic speckle pattern interferometry) [20]	0.5μm	high	Need CCD camera
4	Moiré interferometry [21]	Nanometer range	high	Same as above
5	LVDT (linear variable differential transformer) [18]	A fraction of μm	Sensitive to EM interference	Need demodulator
6	SAWR (Surface Acoustic Wave Resonator) [19]	-442HZ/ με	poor	Need network analyzer
7	FBG (fiber Bragg grating) [20, 21]	0.06%ε	High	Need integrator
8	Capacitive strain sensor [17]	0.02 Pf/με	poor	Need additional circuit

The deformation value increases with the rise of the power loss which demonstrates a liner relationship.

4 Detection methods

The work described above shows that thermal stress results in a much larger deformation in the groove of the PP-IGBT lid compared to the clamping force. Based on the relationship between the temperature and deformation, the status of the device can be monitored by measuring this deformation. Fig. 4 shows the comprehensive relationship between the deformation and condition of the device, where the electrical, thermal and mechanical field are all considered for analyzing the deformation. The switch operation and collector current are the main factor in the electrical field since they affect the power dissipation which is the thermal source for temperature variation. In contract, high junction temperature affects the electrical performance, also, the mechanical characteristics. The pressure distribution is the key parameter that affects both the electrical and thermal field and generated by the external clamping force. The combined effect from the three coupled fields make the contribution to the deformation which is selected as the indicator of the condition monitoring for the device. Therefore, the appropriate methods for measuring the deformation is of importance to achieve condition monitoring of PP-IGBT. Table 3 shows several commercial-available deformation sensors on the market.

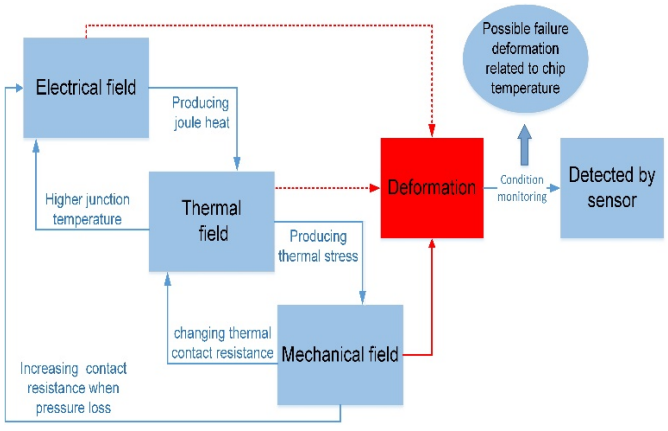

Fig. 4 Diagram of deformation affected by the coupled model

As shown in Fig.3(c), the deformation ranges from 38 to 72 μm with the increase of power dissipation, thus, some limitations have been identified to choose the appropriate detection methods. Firstly, the space is in the millimeter range due to the physical position of the press pack cell and the heat-sink. In addition, the grove shares the applied voltage potential and as PP-IGBT are switching devices and high immunity to electromagnetic interference is also required. Finally, the absolute value of the deformation remains small compared to the lid size, which means high measuring accuracy and sensitivity are required. According to these practical conditions, several market-available sensors for deformation detection have been compared and analyzed in terms of sensitivity, dimension, immunity, complexity and detecting principle.

From this table, the investigated sensors can be generally categorized into different types according to the output signals, such as the voltage, optical, frequency and so on. Strain gauge, capacitive strain sensor and LVDT are all measuring the deformation based on the change of the output voltage [16-18], the sensitivity of the three sensors is enough to detect the micrometer change and the strain gauge sensors have advantages in cost, however, the immunity to the electro-magnetic field for such types of sensors is relatively poor but it can be overcome by adding insulator material. SAWR sensor detects the deformation by measuring the change of the frequency and velocity for a produced acoustic wave. The immunity to electro-magnetic, however, remains poor and the connection between the sensor and the device is difficult [19]. The long-gauge-length fiber optical sensor and FBG sensor are fiber optical sensor [20], the immunity is high enough as well as the sensitivity. Moiré interferometry sensor and ESPI sensor are based on the interferometry principle to detect the deformation [20, 21]. The sensitivity and immunity can basically meet the requirements, but the additional device is required, and the cost is extremely high for the practical applications. Therefore, two feasible sensors are selected for a further investigation: the strain gauge sensor and FBG sensor. The basic principle of the strain gauge sensor is that the output voltage is proportional to the deformation of the transducer when detecting the deformation. Normally, the Wheatstone bridge is constructed with a voltage or current excitation source to measure the small change in resistance.

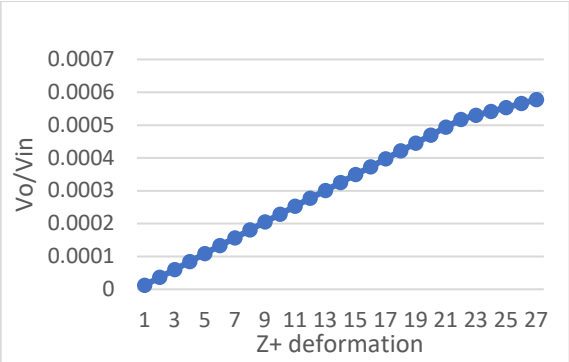

Fig. 5 output voltage ratio based on the Z+ deformation

The gauge factor (GF) which is the typical ratio of the change in electrical resistance to the fractional change in strain is typically around 2 in the commercial market. Equation (4) shows the definition of GF [16].

$$GF = \frac{\Delta R/R}{\Delta L/L} \tag{4}$$

Fig.5 shows the simulation results of the strain gauge sensor by applying the deformation values. The output voltage ratio is quite small, and the normal voltage sensor cannot detect the voltage in this range. Also, there are relatively large tolerances in resistors caused by the manufacturing process. Therefore, this solution cannot be recommended.

Based on the cost, sensitivity and the complexity of installation, FBG shows unique features for deformation measurement of PP-IGBTs. FBG sensor is a grating-based sensor which is a simple and intrinsic sensor. It has several advantages such as: small size, good corrosion resistance, immune to electromagnetic interference, low thermal conductivity and distributed measurement. Therefore, this type of sensor is particularly suitable for PP-IGBTs. Fig. 6 shows the principle of FBG sensor. The basic principle of the FBG-based sensor system is to detect the shift of the reflection or transmission center wavelength (Bragg) by an optical spectrum analyzer, the shift is related to the amount of strain. Equation (5) developed for vacuum, describes the Bragg wavelength of the FBG λ_B is the function of the periodicity of the grating Λ and the effective refractive index of the fiber n_{eff}.

$$\lambda_B = 2n_{eff}\Lambda \tag{5}$$

In order to calculate the sensitivity of the Bragg wavelength with the strain, equation (6) is obtained that the sensitivity with strain is the partial derivative of (5) with respect to displacement:

$$\frac{\Delta\lambda_B}{\lambda_B} = 2n_{eff}\frac{\partial\Lambda}{\partial L} + 2\Lambda\frac{\partial n_{eff}}{\partial L} \tag{6}$$

The first term in (6) is the strain of the grating period due to the extension of the fiber, and the second term is the variation of the index of refraction caused by the strain. The expression (7) describes the classical form of the Bragg wavelength displacement with the strain which combined both phenomena, where ε_{FBG} is the longitudinal strain of the grating, and the ρ_e is the photo-elastic coefficient.

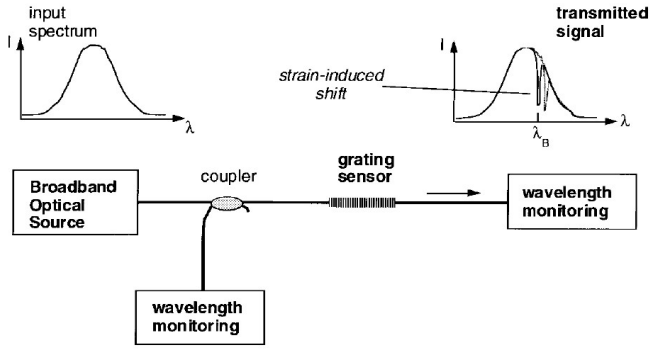

Fig. 6 Basic principle of Bragg grating-based sensor system [21]

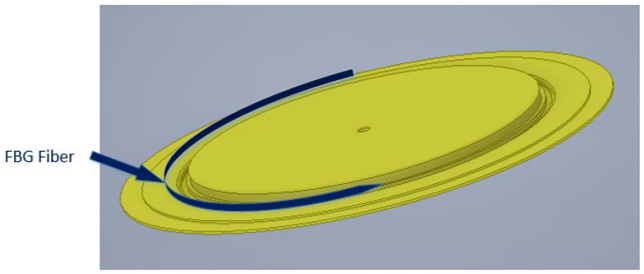

Fig. 7 Positioning of FBG onto the copper collector lid

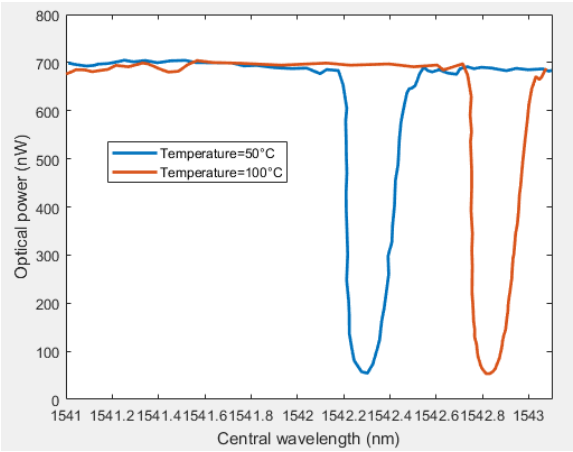

Fig. 8 Simplified FBG results of the change for the central wavelength

$$\frac{\Delta\lambda_B}{\lambda_B} = (1-\rho_e)\varepsilon_{FBG} \tag{7}$$

In terms of validating applying the FBG sensor for PP IGBT, the sensitivity needs to be calculated based on (7). According to the selected tunable laser source, the generated wavelength ranges from 1240nm to 1680nm, then the theoretical grating sensitivities to the strain is in the range of 0.96pm/$\mu\varepsilon$ to 1.31 pm/$\mu\varepsilon$ [19] which can be detected by the commercial spectrum analyzer.

Fig. 7 shows the positioning of applying FBG fiber to measure the deformation of the lid. The idea is to wrap the fiber around the groove. The most common application for utilizing PP-IGBTs is HVDC, and the typical structure to connect the devices in series to form a stack to use. Normally there are hundreds of PP-IGBTs in series connection in one stack. As the FBG sensors can be fabricated in a string to measure distributed multi-points, this is very suitable to be employed

in the HVDC applications. Also, the cost of the FBG measurement system including the laser source and spectrum analyser is insignificant compared to the entire HVDC system. Fig.8 demonstrates a simplified example of applying FBG to the PP-IGBT to measure the deformation, where the change of the central wavelength can be detected under different conditions.

5 Conclusion

To find an appropriate parameter for condition monitoring for PP-IGBTs, a thermal-mechanical field analysis of an PP IGBT under steady current operation condition was performed using finite element simulation. The deformation of the groove in the lid of the PP-IGBT was identified as a new condition monitoring parameter as the paper established a linear relationship between the deformation of the groove and the thermal distribution caused by IGBT chips. A study on possible detection methods for deformation measurement are reviewed and it is concluded that the FBG sensor is the most appropriate sensor to detect the deformation.

References

[1] T. K. Vrana and S. Energi, "Review of HVDC component ratings: XLPE cables and VSC converters," *2016 IEEE International Energy Conference (ENERGYCON)*, Leuven, 2016, pp. 1-6.

[2] P. Bordignon, H. Zhang, W. Shi, N. Serbia and A. Coffetti, "HV submodule technology based on press pack IGBT for largest scale VSC-HVDC application," *12th IET International Conference on AC and DC Power Transmission (ACDC 2016),* Beijing, 2016, pp. 1-6.

[3] IEEE T&D committee 2000 – CIGRE WG-B4 04 2003

[4] F. Wakeman, J. Pitman and S. Steinhoff, "Long term short-circuit stability in Press-pack IGBTs," *2016 18th European Conference on Power Electronics and Applications (EPE'16 ECCE Europe),* Karlsruhe, 2016, pp. 1-10.

[5] Dai S, Song X, Li G, Ji B, Pickert V, Electromagnetic analysis of press pack IEGT with transient skin and proximity effects, *International Exhibition and Conference for Power Electronics, Intelligent Motion, Renewable Energy and Energy Management (PCIM-Asia),* Shanghai, China, 26-28 June 2019.

[6] Chen H, Cao W, Bordignon P, et al. Design and testing of the World's first single-level press-pack IGBT based submodule for MMC VSC HVDC applications[C]//*Energy Conversion Congress and Exposition (ECCE),* 2015 IEEE. IEEE, 2015: 3359-3366.

[7] T. Poller, J. Lutz, S. D'Arco and M. Hernes, "Determination of the thermal and electrical contact resistance in press-pack IGBTs," *2013 15th European Conference on Power Electronics and Applications (EPE),* Lille, 2013, pp. 1-9.

[8] Lukas Tinschert, Atle Rygg Årdal, Tilo Poller, Marco Bohlländer, Magnar Hernes, Josef Lutz, Possible failure modes in Press-Pack IGBTs, Microelectronics Reliability, Volume 55, Issue 6, 2015, Pages 903-911,

[9] E. Deng, Z. Zhao, Z. Lin, R. Han and Y. Huang, "Influence of Temperature on the Pressure Distribution Within Press Pack IGBTs," in *IEEE Transactions on Power Electronics*, vol. 33, no. 7, pp. 6048-6059, July 2018.

[10] Poller, T., D'Arco, S., Hernes, M., Ardal, A. R., & Lutz, J.: Influence of the clamping pressure on the electrical, thermal and mechanical behavior of press-pack IGBTs [J]. *Microelectronics Reliability,* 53.2013, 1755–1759

[11] Mandeya R, Chen C, Pickert V, Naayagi RT, Pre-threshold voltage as a low component count Temperature Sensitive Electrical Parameter without Self-Heating, *IEEE Transactions on Power Electronics,* 2018, 33(4), 2782-2791.

[12] M. Gu *et al*., "Condition Monitoring of High Voltage IGBT Devices Based on Controllable RF Oscillations," *2019 31st International Symposium on Power Semiconductor Devices and ICs (ISPSD)*, Shanghai, China, 2019, pp. 355-358.

[13] H. Li, R. Yao, W. Lai, H. Ren and J. Li, "Modeling and Analysis on Overall Fatigue Failure Evolution of Press-Pack IGBT Device," in IEEE Transactions on Electron Devices, vol. 66, no. 3, pp. 1435-1443, March 2019.

[14] Recommendations regarding mechanical clamping of Press Pack High Power Semiconductors， ABB.

[15] Oh H, Han B, McCluskey P, et al. Physics-of-failure, condition monitoring, and prognostics of insulated gate bipolar transistor modules: A review[J]. *IEEE Transactions on power electronics,* 2015, 30(5): 2413-2426.

[16] Strain gauge measurement – National Instruments application note 078

[17] Aebersold, J., Walsh, K., Crain, M., Voor, M., Martin, M., Hnat, W., Lin, J., Jackson, D., and Naber, J.: Design, modeling, fabrication and testing of a MEMS capacitive bending strain sensor, *J. Phys. Conf. Ser.,* 34, 124–129, 2006.

[18] Chia-Chang Tong, Chi-Jui Chao, Tzu-Yuan Lin, Wei-Nan Lin and Chun-Ting Yang, "A Kalman filter approach to LVDT-based heat deformation test," *2008 IEEE International Conference on Systems,* Man and Cybernetics, Singapore, 2008, pp. 1861-1865.

[19] B. Donohoe, D. Geraghty, G. E. O'Donnell and R. Stoney, "Packaging Considerations for a Surface Acoustic Wave Strain Sensor," *in IEEE Sensors Journal,* vol. 12, no. 5, pp. 922-925, May 2012.

[20] S. M. Avery and R. D. Lorenz, "In Situ Measurement of Wire-Bond Strain in Electrically Active Power Semiconductors," *in IEEE Transactions on Industry Applications,* vol. 49, no. 2, pp. 973-981, March-April 2013.

[21] A. D. Kersey, M. A. Davis, H. J. Patrick et al., "Fiber grating sensors," *Journal of Lightwave Technology,* vol. 15, no. 8, pp. 1442–1462, 1997.